

Bayesian Optimization for Non-Cooperative Game-Based Radio Resource Management

Yunchuan Zhang*, Jiechen Chen[†], Junshuo Liu[‡] and Robert C. Qiu[‡]

*School of Information Engineering, Wuhan University of Technology, Wuhan, China

[†]Department of Engineering, King's College London, London, UK

[‡]School of Electronic Information and Communications, Huazhong University of Science and Technology, Wuhan, China

Email: {yunchuan.zhang, jiechen.chen}@kcl.ac.uk, {junshuo_liu, caiming}@hust.edu.cn

Abstract—Radio resource management in modern cellular networks often calls for the optimization of complex utility functions that are potentially conflicting between different base stations (BSs). Coordinating the resource allocation strategies efficiently across BSs to ensure stable network service poses significant challenges, especially when each utility is accessible only via costly, black-box evaluations. This paper considers formulating the resource allocation among spectrum sharing BSs as a non-cooperative game, with the goal of aligning their allocation incentives toward a stable outcome. To address this challenge, we propose PPR-UCB, a novel Bayesian optimization (BO) strategy that learns from sequential decision-evaluation pairs to approximate pure Nash equilibrium (PNE) solutions. PPR-UCB applies martingale techniques to Gaussian process (GP) surrogates and constructs high probability confidence bounds for utilities uncertainty quantification. Experiments on downlink transmission power allocation in a multi-cell multi-antenna system demonstrate the efficiency of PPR-UCB in identifying effective equilibrium solutions within a few data samples.

Index Terms—Bayesian optimization, radio resource management, Nash equilibrium, uncertainty quantification

I. INTRODUCTION

Radio resource management of modern cellular communication system requires the optimization of complex utilities which may involve potential *conflicts* between different segments of the network. To ensure stable network operations during optimizations, one promising way is via game-theoretic methods [1]. For instance, heterogeneous spectrum providers configure the exclusion zones in dynamic spectrum access (DSA) networks via analyzing *Nash equilibrium* (NE) in a non-cooperative game [2], but conventional mathematical programming methods for NE often require analytical expressions of the utilities which may not be available in practice. When the utilities are in the form of *black-box* functions, the evaluation of a NE must rely on querying the utilities of each involved entity.

For concreteness, this paper investigates the downlink transmission power control game with *unknown* utilities in a multi-cell multi-antenna communication system [3]. As illustrated in Fig. 1, a central optimizer assigns a set of transmission power actions to different *players*, representing spectrum sharing BSs managed by mobile network operators (MNOs). The goal is to design an optimization policy that ensures no players have incentives to deviate from the allocated power actions. Thus,

the suggested action set aligns closely with the individual rationality of the players. This equilibrium solution ensures a stable operation of the network as the players strictly adhere to the allocated actions of the central optimizer.

To tackle the non-cooperative games with black-box utilities, prior works applied reinforcement learning (RL) for identifying NE solutions [4], [5], and provided practical use cases in communications systems [6], [7]. In particular, reference [8] introduced a fully distributed deep RL architecture for DSA that can be flexibly adapted to general complex real-world settings. However, RL algorithms typically rely on large amounts of utilities observations which may incur undesirable evaluation costs on computational overhead or communications latency.

Bayesian optimization (BO) is a common sample-efficient framework for *costly-to-evaluate* black-box optimization problems [9], and its variants have been widely applied to applications in wireless systems [10], [11]. The first attempt to seek for NE via BO can be found in [12]; while reference [13] provided a formal NE regret guarantee for using BO with confidence sets. However, these studies require making strong assumptions on the function space knowledge regarding the utilities and evaluating the NP-hard maximal information gain metrics which are impractical in real-world scenarios.

In this paper, we introduce a novel BO policy, namely *prior-posterior ratio upper confidence bounds* (PPR-UCB) that aims at approximating a *pure Nash equilibrium* (PNE) solution in a non-cooperative transmission power control game. The main contributions are as follows.

- We introduce PPR-UCB, a novel BO policy tailored for evaluation of approximate PNEs in general-sum games with black-box utility functions. PPR-UCB adopts martingale techniques to efficiently construct confidence sets for the probabilistic utilities and deviation incentives of each involved players.
- We provide a coverage analysis of the *any-time valid* confidence sets constructed by the prior-posterior ratio martingales. The theoretical results demonstrates the reliability of the proposed PPR-UCB policy.
- We validate the performance of the proposed PPR-UCB in a multi-cell cellular network. Empirical results for the non-cooperative power control game provide insights

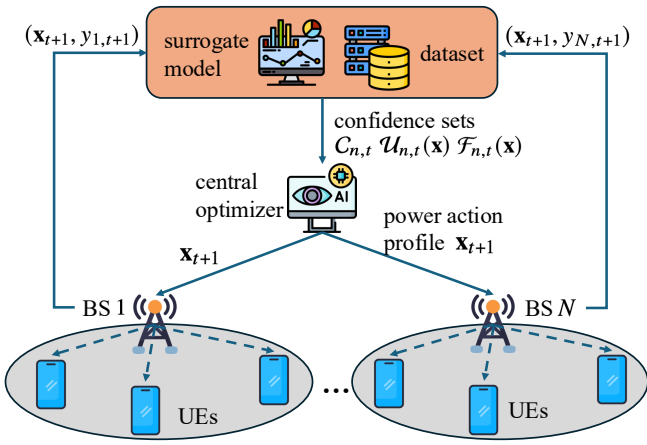


Fig. 1. This paper studies a setting in which a central optimizer uses BO to approximate the pure Nash equilibrium (PNE) for a non-cooperative downlink transmission power control game with costly-to-evaluate black-box utility functions of N BSs. At any time $t + 1$, the central optimizer assigns an action profile \mathbf{x}_{t+1} to all BSs. As a result, the optimizer receives noisy utility feedback $y_{n,t}$ about the corresponding utility value $u_n(\mathbf{x}_{t+1})$ for all BSs $n \in \mathcal{N}$. The goal is to approach a solution in the ϵ -PNE set (5), where $\epsilon \geq 0$ represents the dissatisfaction tolerance.

into the potential benefits of using BO for conflicts management in communications systems.

II. PROBLEM FORMULATION

To exemplify the application of the proposed sequential black-box optimization policy, we consider the non-cooperative game-based downlink transmission power control problem studied in [3]. The targeting cellular communication network consists of N cells with one BS, each belonging to a private MNO that provides service for M user equipments (UEs). The MNOs in the network operates on a shared frequency band.

As shown in Fig. 1, the central coordinator is tasked with selection of an action profile $\mathbf{x} = [\mathbf{x}_1, \dots, \mathbf{x}_N] \in \mathcal{X}$ for N BSs, where $\mathbf{x}_n = [x_{n,1}, \dots, x_{n,M}] \subset \mathbb{R}^M$ represents the selected power action for BS $n \in \mathcal{N} = [1, \dots, N]$ with each entry $x_{n,m}$ describing the downlink transmission power to its serving UE $m \in \mathcal{M} = [1, \dots, M]$. The propagation channel matrix between BS n and any UE m associated with BS n' is modeled as

$$\mathbf{H}_{n,n'(m)} = 10^{\frac{-\text{PL}(d_{n,n'(m)})}{20}} \beta_{n,n'(m)} \mathbf{G}_{n,n'(m)}, \quad (1)$$

where the pathloss $\text{PL}(d_{n,n'(m)})$ in dB is a function of the distance from BS n to UE m served by BS n' ; the slow fading factor $\beta_{n,n'(m)}$ depends on whether the corresponding transmission is in line-of-sight (LOS) or non-line-of-sight (NLOS) as specified in 3GPP TR 38.901 [14]; and the fast fading $\mathbf{G}_{n,n'(m)}$ in the form of $N_R \times N_T$ matrix has i.i.d. complex Gaussian entries with N_T being the number of transmit antennas at each BS and N_R being the number of receiving antennas at each UE.

Each MNO is *self-interested*, and attempts to maximize the utility of its own BS. Specifically, the utility function for BS $n \in \mathcal{N}$ at the assigned action profile \mathbf{x} is described by the

discounted sum spectral efficiency across the associated UEs, which is defined as

$$u_n(\mathbf{x}) = -\lambda \left(\sum_{m=1}^M x_{n,m} \right) + \left[\sum_{m=1}^M \log |\mathbf{I} + x_{n,m} \mathbf{\Gamma}_{n,n(m)}^{-1}(\mathbf{x}) \mathbf{H}_{n,n(m)} \mathbf{H}_{n,n(m)}^H| \right], \quad (2)$$

where $\lambda \geq 0$ is a non-negative discount factor; \mathbf{I} is the $N_R \times N_R$ identity matrix; and $\mathbf{\Gamma}_{n,n(m)}^{-1}(\mathbf{x})$ represents the $N_R \times N_R$ interference-plus-noise covariance matrix for the transmission from BS n to its serving UE m , i.e.,

$$\mathbf{\Gamma}_{n,n(m)}^{-1}(\mathbf{x}) = 10^{\frac{\sigma_h^2}{10}} \mathbf{I} + \sum_{m'=1, m' \neq m}^M x_{n,m'} \mathbf{H}_{n,n(m')} \mathbf{H}_{n,n(m')}^H + \sum_{n'=1, n' \neq n}^N \sum_{m=1}^M x_{n',m} \mathbf{H}_{n',n'(m)} \mathbf{H}_{n',n'(m)}^H \quad (3)$$

with σ_h^2 being the channel noise power in dB scale.

Upon receiving the action profile \mathbf{x} from the central coordinator, each BS $n \in \mathcal{N}$ quantifies its *dissatisfaction* on the assigned action \mathbf{x} via the non-negative regret

$$f_n(\mathbf{x}) = \max_{\mathbf{x}'_n} u_n(\mathbf{x}'_n, \mathbf{x}_{-n}) - u_n(\mathbf{x}) \geq 0, \quad (4)$$

where \mathbf{x}_{-n} represents the actions taken by all BSs except for BS n . The dissatisfaction (4) indicates that any BS n may unilaterally deviate from the assigned action \mathbf{x}_n if doing so can improve its utility. These deviation incentives across all BSs degrade the *stability* of the network operations. To this end, the goal of the central optimizer is to seek for a set of ϵ -PNE solutions $\mathbf{x}^{(\epsilon)}$ defined as

$$\mathcal{X}^{(\epsilon)} := \{\mathbf{x}^{(\epsilon)} \in \mathcal{X} | f_n(\mathbf{x}^{(\epsilon)}) \leq \epsilon \text{ for } n \in \mathcal{N}\}, \quad (5)$$

for some tolerance parameter $\epsilon \geq 0$.

Evaluating the utility functions (2) and the regret (4) for all feasible action profiles to find the ϵ -PNE set (5) is intractable as the scale of the network increases. Therefore, we adopt an online learning-based optimizer that sequentially selects an action profile \mathbf{x}_t at time t , and receives the noisy observations from each BS $n \in \mathcal{N}$, i.e.,

$$y_{n,t} = u_n(\mathbf{x}_t) + z_{n,t}, \quad (6)$$

where the observation noise variables $z_{n,t} \sim \mathcal{N}(0, \sigma^2)$ are independent across all BSs. The decision-making process relies on the collections of previous observations

$$\mathcal{D}_{n,t-1} = \{(\mathbf{x}_1, y_{n,1}), \dots, (\mathbf{x}_{t-1}, y_{n,t-1})\} \quad (7)$$

from all BSs.

III. BO FOR NON-COOPERATIVE GAMES

In this section, we introduce *prior-posterior ratio upper confidence bounds* (PPR-UCB) by first presenting the confidence sets construction for utilities and regret, and then detailing the action profiles acquisition process. We start with a brief review of the surrogate model adopted in BO policy.

A. Gaussian Process

As anticipated, BO does not require a precise expression of the utility function for calculating the ϵ -PNE set (5), but works on black-box evaluations of the utility that is modeled by a *probabilistic surrogate model*. Gaussian process (GP) is the typical model of choice as it provides analytical posterior inference with small datasets.

Specifically, for each BS n , a separate GP is deployed at the central optimizer to model the individual utility function $u_n(\mathbf{x})$ by assuming that, for any collection $\mathbf{X}_t = [\mathbf{x}_1, \dots, \mathbf{x}_t]^\top$ of action profiles, the corresponding utility observations $\mathbf{y}_{n,t} = [y_{n,1}, \dots, y_{n,t}]^\top$ follow a multivariate Gaussian distribution $\mathcal{N}(\mathbf{0}, \mathbf{K}(\mathbf{X}_t))$, with $t \times 1$ zero mean vector $\mathbf{0}$, and $t \times t$ covariance matrix $\mathbf{K}(\mathbf{X}_t)$ given by

$$\mathbf{K}(\mathbf{X}_t) = \begin{bmatrix} k(\mathbf{x}_1, \mathbf{x}_1) & \dots & k(\mathbf{x}_1, \mathbf{x}_t) \\ \vdots & \ddots & \vdots \\ k(\mathbf{x}_{t-1}, \mathbf{x}_1) & \dots & k(\mathbf{x}_{t-1}, \mathbf{x}_t) \end{bmatrix}, \quad (8)$$

where each entry is obtained via a positive semidefinite kernel function $k(\mathbf{x}, \mathbf{x}')$. Intuitively, the role of the kernel function is to measure the similarity between inputs \mathbf{x} and \mathbf{x}' in terms of the respective utility values. The kernel function may be chosen, for instance, as the radial basis function (RBF) kernel

$$k(\mathbf{x}, \mathbf{x}') = \exp\left(-\frac{\|\mathbf{x} - \mathbf{x}'\|^2}{2l^2}\right), \quad (9)$$

where the lengthscale parameter $l > 0$ controls the smoothness of the kernel function.

Given the collected dataset $\mathcal{D}_{n,t}$ in (7), the posterior distribution of utility value $u_n(\mathbf{x})$ at any action profile \mathbf{x} is a Gaussian distribution

$$p(u_n(\mathbf{x})|\mathcal{D}_{n,t}) = \mathcal{N}(\mu_{n,t}(\mathbf{x}), \sigma_t^2(\mathbf{x})), \quad (10)$$

where

$$\mu_{n,t}(\mathbf{x}) = \mathbf{k}_t(\mathbf{x})^\top (\mathbf{K}(\mathbf{X}_t) + \sigma^2 \mathbf{I})^{-1} \mathbf{y}_{n,t}, \quad (11a)$$

$$\sigma_t^2(\mathbf{x}) = k(\mathbf{x}, \mathbf{x}) - \mathbf{k}_t(\mathbf{x})^\top (\mathbf{K}(\mathbf{X}_t) + \sigma^2 \mathbf{I})^{-1} \mathbf{k}_t(\mathbf{x}), \quad (11b)$$

with the $t \times 1$ cross-variance vector $\mathbf{k}_t(\mathbf{x}) = [k(\mathbf{x}, \mathbf{x}_1), \dots, k(\mathbf{x}, \mathbf{x}_t)]^\top$. Note that, the GP posterior variance $\sigma_t^2(\mathbf{x})$ in (11b) is the same across all players since it only depends on the previously selected action profiles \mathbf{X}_t and the current action profile \mathbf{x} to be measured.

B. Prior-Posterior Ratio Confidence Sets

To quantify the residual uncertainty on the inference of the utility function $u_n(\mathbf{x})$ at any candidate action profile \mathbf{x} , PPR-UCB constructs the confidence sets for the model parameters with probabilistic coverage guarantee. To proceed, we make the following regularity assumption on the utility functions of each BS $n \in \mathcal{N}$.

Assumption 1 (Probabilistic Utility Function). *The utility function $u_n(\mathbf{x})$ at each BS n can be decomposed as*

$$u_n(\mathbf{x}) = \psi_n(\mathbf{x})^\top \boldsymbol{\theta}_n^*, \quad (12)$$

where $\psi_n(\mathbf{x})$ is a $D \times 1$ feature vector; and the unknown parameters vector $\boldsymbol{\theta}_n^* \in \mathbb{R}^{D \times 1}$ is drawn from an isotropic Gaussian prior distribution $p(\boldsymbol{\theta})$, i.e., $\boldsymbol{\theta}_n^* \sim \mathcal{N}(\mathbf{0}, \mathbf{I}_D)$. The vectors $\{\boldsymbol{\theta}_n^*\}_{n \in \mathcal{N}}$ are mutually independent.

Assumption 1 can serve as an arbitrarily accurate approximation of the typical assumption that the utility functions are drawn in an i.i.d. manner from the GP model in (10) with RBF kernel [15]. In fact, the RBF kernel can be approximated arbitrarily well by the inner product

$$k(\mathbf{x}, \mathbf{x}') \approx \psi_n(\mathbf{x})^\top \psi_n(\mathbf{x}') \quad (13)$$

with a sufficiently high-dimensional feature vector $\psi_n(\mathbf{x}) \in \mathbb{R}^{D \times 1}$. In practice, consider the random Fourier features (RFFs)

$$\psi_n(\mathbf{x}) = [\sqrt{2/D} \cos(\mathbf{s}_{n,i}^\top \mathbf{x} + b_{n,i})]_{i=1}^D, \quad (14)$$

with $d \times 1$ vectors $\mathbf{s}_{n,i}$ drawn i.i.d. from $\mathcal{N}(0, 2l\mathbf{I}_d)$ and scalars $b_{n,i}$ sampled i.i.d. from the uniform distribution over the interval $[0, 2\pi]$. With an increasing dimension $D \rightarrow \infty$ of the RFFs, the approximation error in (13) vanishes with high probability [15].

At each time t , PPR-UCB evaluates the posterior distribution of parameters vector $\boldsymbol{\theta}_n$ for BS $n \in \mathcal{N}$ under Assumption 1 as follows

$$p(\boldsymbol{\theta}_n|\mathcal{D}_{n,t}) \propto p(\boldsymbol{\theta}_n)p(\mathcal{D}_{n,t}|\boldsymbol{\theta}_n) = \mathcal{N}(\boldsymbol{\mu}_{n,t}, \sigma^2 \boldsymbol{\Sigma}_{n,t}^{-1}), \quad (15)$$

where

$$\boldsymbol{\mu}_{n,t} = \boldsymbol{\Sigma}_{n,t}^{-1} \boldsymbol{\Psi}_{n,t}^\top \mathbf{y}_{n,t}, \quad (16a)$$

$$\boldsymbol{\Sigma}_{n,t} = \boldsymbol{\Psi}_{n,t}^\top \boldsymbol{\Psi}_{n,t} + \sigma^2 \mathbf{I}_D \quad (16b)$$

with $\boldsymbol{\Psi}_{n,t} = [\psi_n(\mathbf{x}_1), \dots, \psi_n(\mathbf{x}_t)]^\top$ being the $t \times D$ matrix of the feature vectors. Therefore, the mean and variance of the GP posterior distribution (10) for the utility value $u_n(\mathbf{x})$ can be obtained as

$$\mu_{n,t}(\mathbf{x}) = \psi_n(\mathbf{x})^\top \boldsymbol{\Sigma}_{n,t}^{-1} \boldsymbol{\Psi}_{n,t}^\top \mathbf{y}_{n,t}, \quad (17a)$$

$$\begin{aligned} \sigma_t^2(\mathbf{x}) = & \psi_n(\mathbf{x})^\top \psi_n(\mathbf{x}) \\ & - \psi_n(\mathbf{x})^\top \boldsymbol{\Psi}_{n,t}^\top (\boldsymbol{\Psi}_{n,t}^\top \boldsymbol{\Psi}_{n,t} + \sigma^2 \mathbf{I}_D)^{-1} \boldsymbol{\Psi}_{n,t} \psi_n(\mathbf{x}). \end{aligned} \quad (17b)$$

Using the posterior (15) of the parameters vector $\boldsymbol{\theta}_n$ for BS n at each time t , PPR-UCB evaluates the prior-posterior ratio

$$\begin{aligned} \ell_{n,t}(\boldsymbol{\theta}_n) = & \frac{p(\boldsymbol{\theta}_n)}{p(\boldsymbol{\theta}_n|\mathcal{D}_{n,t})} \\ = & \frac{\sigma^D}{\sqrt{\det(\boldsymbol{\Sigma}_{n,t})}} \exp\left(-\frac{1}{2}\|\boldsymbol{\theta}_n\|^2\right. \\ & \left. + \frac{1}{2\sigma^2}(\boldsymbol{\theta}_n - \boldsymbol{\mu}_{n,t})^\top \boldsymbol{\Sigma}_{n,t}(\boldsymbol{\theta}_n - \boldsymbol{\mu}_{n,t})\right), \end{aligned} \quad (18)$$

where $\det(\boldsymbol{\Sigma}_{n,t})$ is the determinant of covariance matrix $\boldsymbol{\Sigma}_{n,t}$. Smaller values of the prior-posterior ratio indicates that the parameters vector $\boldsymbol{\theta}_n$ has a large posterior probability density, suggesting that $\boldsymbol{\theta}_n$ aligns better with the evidence provided by the collected data under Assumption 1.

At any time $t \geq 1$, using the prior-posterior ratio in (18), PPR-UCB builds confidence sets for parameters vector θ_n as

$$\begin{aligned} C_{n,t} &= \{\theta_n | \ell_{n,t}(\theta_n) \leq 1/\delta\} \\ &= \{\theta_n | (\theta_n - \mu_{n,t})^\top \Sigma_{n,t} (\theta_n - \mu_{n,t}) - \|\theta_n\|^2 \\ &\quad \leq 2[\ln(\det(\Sigma_{n,t})) - \ln(\sigma^D \delta)]\} \end{aligned} \quad (19)$$

for all players n , where $\delta \in (0, 1]$ is a hyperparameter. The confidence set (19) indicates that with high probability, i.e., δ is sufficiently small, the mean estimate $\mu_{n,t}$ is included.

Lemma 1 (Utility Parameters Coverage Guarantee of PPR-UCB). *Under Assumption 1, the confidence set (19) is anytime valid at level $1 - \delta$ in the sense that it includes the ground truth parameters θ_n^* with probability no smaller than $1 - \delta$ for all time $t \geq 1$:*

$$\Pr(\theta_n^* \in C_{n,t}, \text{ for all } t \geq 1) \geq 1 - \delta. \quad (20)$$

In (20), the probability is evaluated with respect to the ground truth distribution

$$p(\mathcal{D}_{n,t} | \theta_n^*) = \prod_{t'=1}^t p(y_{n,t'} | \mathbf{x}_{t'}, \theta_n^*). \quad (21)$$

Proof. By taking the expectation of the prior-posterior ratio $\ell_{n,t}(\theta_n^*)$ conditioned on the collected dataset $\mathcal{D}_{n,t-1}$ and applying Fubini's theorem, we have

$$\begin{aligned} &\mathbb{E}_{p(y|\mathbf{x}_t, \theta_n^*)} [\ell_{n,t}(\theta_n^*) | \mathcal{D}_{n,t-1}] \\ &= \mathbb{E}_{p(y|\mathbf{x}_t, \theta_n^*)} \left[\prod_{t'=1}^t \frac{\mathbb{E}_{p(\theta_n | \mathcal{D}_{n,t})} p(y_{n,t'} | \mathbf{x}_{t'}, \theta_n)}{p(y_{n,t'} | \mathbf{x}_{t'}, \theta_n^*)} \middle| \mathcal{D}_{n,t-1} \right] \end{aligned} \quad (22)$$

$$\begin{aligned} &= \mathbb{E}_{p(\theta_n | \mathcal{D}_{n,t})} \left[\ell_{n,t-1}(\theta_n^*) \mathbb{E}_{p(y|\mathbf{x}_t, \theta_n^*)} \left[\frac{p(y_{n,t} | \mathbf{x}_t, \theta_n)}{p(y_{n,t} | \mathbf{x}_t, \theta_n^*)} \right] \right. \\ &\quad \left. \middle| \mathcal{D}_{n,t-1} \right] \end{aligned} \quad (23)$$

$$\leq \ell_{n,t-1}(\theta_n^*). \quad (24)$$

The inequality (24) shows that the prior-posterior ratio sequence $\{\ell_{n,t}(\theta_n^*)\}_{t \geq 1}$ is a test *supermartingale* for the ground truth distribution $p(\mathcal{D}_{n,t} | \theta_n^*)$. By applying the Ville's inequality [16], we have

$$\Pr(\theta_n^* \in C_{n,t}, \text{ for all } t \geq 1) = 1 - \Pr(\exists \theta_n^*, \ell_{n,t}(\theta_n^*) > 1/\delta) \quad (25)$$

$$\geq 1 - \delta \mathbb{E}[\ell_{n,t}(\theta_n^*)] \quad (26)$$

$$= 1 - \delta, \quad (27)$$

which completes the proof. \square

Using the confidence set $C_{n,t}$ in (19), PPR-UCB then evaluates the confidence sets for the utility functions $u_n(\mathbf{x})$ and regret $f_n(\mathbf{x})$ for all BSs.

Algorithm 1: PPR-UCB

Input Total number of iterations T , lengthscale l , parameter δ
Output Optimized solution \mathbf{x}^*

- 1 Initialize observation dataset $\mathcal{D}_{n,0} = \emptyset$ for all BSs, iteration $t = 0$
- 2 **while** $t \leq T$ **do**
- 3 Evaluate the prior-posterior ratio $\ell_{n,t}(\theta_n)$ as in (18) for all BSs
- 4 Build the confidence set $C_{n,t}$ as in (19)
- 5 Obtain the utility confidence intervals $\{\mathcal{U}_{n,t}(\mathbf{x})\}_{n \in \mathcal{N}}$ as in (28)
- 6 Obtain the regret confidence intervals $\{\mathcal{F}_{n,t}(\mathbf{x})\}_{n \in \mathcal{N}}$ as in (29)
- 7 Report the action profile $\tilde{\mathbf{x}}_{t+1}$ via (30)
- 8 Select the exploring action profile $\mathbf{x}^{(n_{t+1})}$ via (32)
- 9 Produce the final decision \mathbf{x}_{t+1} via (33)
- 10 Evaluate \mathbf{x}_{t+1} and update datasets as $\mathcal{D}_{n,t+1} = \mathcal{D}_{n,t} \cup (\mathbf{x}_{t+1}, y_{n,t+1})$ for all BSs $n \in \mathcal{N}$
- 11 Update the GP posterior using $\mathcal{D}_{n,t+1}$ as in (17a) and (17b) for all BSs $n \in \mathcal{N}$
- 12 Set iteration index $t = t + 1$
- 13 **end**
- 14 **Return** $\mathbf{x}^* = \mathbf{x}_T$

C. Acquisition Process

For the action profile acquisition process, PPR-UCB starts by evaluating a confidence interval for the utility function $u_n(\mathbf{x})$ of each BS n at time t , which is obtained as

$$\begin{aligned} \mathcal{U}_{n,t}(\mathbf{x}) &= [\check{u}_{n,t}(\mathbf{x}), \hat{u}_{n,t}(\mathbf{x})] \\ &= [\min_{\theta_n \in C_{n,t}} \psi_n(\mathbf{x})^\top \theta_n, \max_{\theta_n \in C_{n,t}} \psi_n(\mathbf{x})^\top \theta_n]. \end{aligned} \quad (28)$$

Notably, unlike conventional confidence intervals-guided BO schemes [17], [18], PPR-UCB does not require perfect knowledge on the utility function space, e.g., reproducing kernel Hilbert space (RKHS) norm. Using the confidence interval $\mathcal{U}_{n,t}(\mathbf{x})$ in (28) for the utility function, PPR-UCB also evaluates the confidence set for the regret $f_n(\mathbf{x})$ in (4) of each BS n as

$$\begin{aligned} \mathcal{F}_{n,t}(\mathbf{x}) &= [\check{f}_{n,t}(\mathbf{x}), \hat{f}_{n,t}(\mathbf{x})] \\ &= \left[\max_{\mathbf{x}'_n} \check{u}_{n,t}(\mathbf{x}'_n, \mathbf{x}_{-n}) - \hat{u}_{n,t}(\mathbf{x}), \right. \\ &\quad \left. \max_{\mathbf{x}'_n} \hat{u}_{n,t}(\mathbf{x}'_n, \mathbf{x}_{-n}) - \check{u}_{n,t}(\mathbf{x}) \right]. \end{aligned} \quad (29)$$

Accordingly, the optimizer reports an action profile $\tilde{\mathbf{x}}_{t+1}$ for possible execution at next time $t + 1$ via

$$\tilde{\mathbf{x}}_{t+1} = \arg \min_{\mathbf{x}} \max_{n \in \mathcal{N}} \check{f}_{n,t}(\mathbf{x}). \quad (30)$$

The intuition behind the reported action profile (30) is to minimize the optimistic estimate $\check{f}_{n,t}(\mathbf{x})$ of the regret (4) obtained by any BS $n \in \mathcal{N}$ that has the strongest incentive to deviate. To allow for exploration, the central optimizer

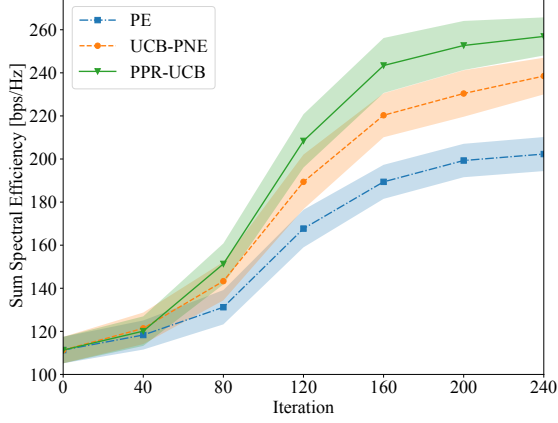


Fig. 2. Sum spectral efficiency against the number of optimization iterations T for PE (blue dash-dotted line), UCB-PNE (orange dashed line), and PPR-UCB with parameter $\delta = 0.05$ (green solid line).

also searches for the BS n_{t+1} with the maximum regret upper bound under the reported action profile $\tilde{\mathbf{x}}_{t+1}$ in (30), i.e.,

$$n_{t+1} = \arg \max_{n \in \mathcal{N}} \hat{f}_{n,t}(\tilde{\mathbf{x}}_{t+1}), \quad (31)$$

and obtains an exploring action profile as

$$\mathbf{x}^{(n_{t+1})} = \left[\tilde{\mathbf{x}}_{-n_{t+1},t+1}, \arg \max_{\mathbf{x}'_{n_{t+1}}} \hat{u}_{n_{t+1},t}(\mathbf{x}'_{n_{t+1}}, \tilde{\mathbf{x}}_{-n_{t+1},t+1}) \right] \quad (32)$$

The exploring action profile $\mathbf{x}^{(n_{t+1})}$ attempts to improve the utility gain for the BS n_{t+1} that the central optimizer believes to have the strongest incentive to deviate from $\tilde{\mathbf{x}}_{t+1}$.

Then, the final decision for the next action profile at time $t+1$ is selected between the reported action profile $\tilde{\mathbf{x}}_{t+1}$ in (30) and the exploring action profile $\mathbf{x}^{(n_{t+1})}$ in (32) that brings higher uncertainty, i.e.,

$$\mathbf{x}_{t+1} = \arg \max_{\mathbf{x} \in \{\tilde{\mathbf{x}}_{t+1}, \mathbf{x}^{(n_{t+1})}\}} \sigma_t^2(\mathbf{x}). \quad (33)$$

The rationale of the choice (33) refers to a double application of the so-called *optimism in the face of uncertainty* (OFU) principle in [19], that is, to encourage maximally reducing uncertainty of potentially promising actions provided by (30) and (32).

The overall procedure of PPR-UCB is summarized in Algorithm 1.

IV. NUMERICAL RESULTS

In this section, we empirically evaluate the performance of the proposed PPR-UCB on the non-cooperative game-based downlink power control problem introduced in Sec. II. Throughout this section, the cellular communication network has $M = 10$ UEs with $N_R = 4$ receiving antennas in each BS with $N_T = 16$ transmit antennas. The propagation pathloss $PL(d_{n,n'}(m))$ and channel fading models in (1) are simulated following the urban microcellular (UMi) street canyon scenario as specified in 3GPP TR 38.901 [14].

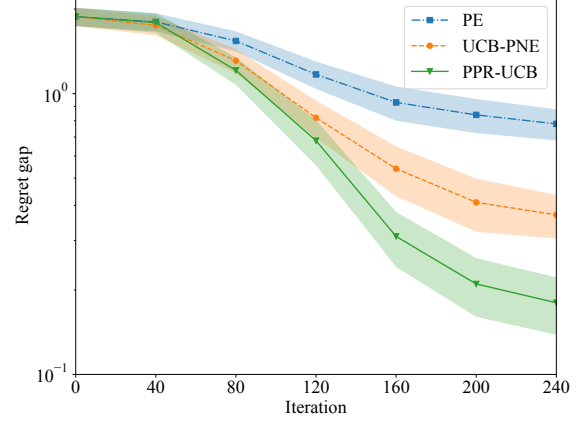


Fig. 3. Regret gap against the number of optimization iterations T for PE (blue dash-dotted line), UCB-PNE (orange dashed line), and PPR-UCB with parameter $\delta = 0.05$ (green solid line).

For the cellular network topology configurations, we consider the service coverage of each BS to be a planar grid with radius being 200 meters, and UEs positions are uniformly generated in the interval $[20, 200]$ meters. The maximum transmit power of each BS is constrained by $\sum_{m=1}^M x_{n,m} \leq p_{\max} = 6.5$ Watt (38.13 dBm); the channel noise power is set to $\sigma_h^2 = -86.46$ dBm; and the discount factor in (2) is set to $\lambda = 0.1$.

We consider the following BO schemes as the benchmarks in all experiments are: 1) *Probability of equilibrium* (PE) [12], which selects action profiles \mathbf{x}_t with the goal of maximizing the probability of obtaining a PNE; and UCB-PNE in [13], which relies on Gaussian bandits optimization techniques [18] to explore the ϵ -PNE solutions. The GPs used in all schemes are configured with lengthscale $l = 0.85$ and observation noise variance $\sigma^2 = 0.67$. The dissatisfaction tolerance level ϵ in (5) is selected as the best achievable level ϵ^* obtained by grid search, which is expressed as

$$\epsilon^* = \inf\{\epsilon \in \mathbb{R} | \mathcal{X}^{(\epsilon)} \neq \emptyset\}. \quad (34)$$

All results are averaged over 100 random realizations of observation noise signals and channel matrices in (1), with error bars to encompass 90% confidence level.

In Fig. 2, we set the parameter $\delta = 0.05$ for PPR-UCB and plot the sum of discounted spectral efficiency across $N = 7$ BSs as a function of the number of optimization iterations T . It is observed that PE obtains the worst performance, since the probability of equilibrium is zero for every action profile when the best achievable tolerance level $\epsilon^* > 0$. Furthermore, our proposed PPR-UCB outperforms UCB-PNE after 40 optimization rounds, and its improvement over all benchmarks is evident as the number of iterations increases, demonstrating the superior data efficiency of PPR-UCB in approximating the ϵ^* -PNE solutions.

In Fig. 3, we evaluate the *regret gap* between ϵ^* with the best achievable ϵ obtained by each scheme, i.e., $\epsilon - \epsilon^*$,

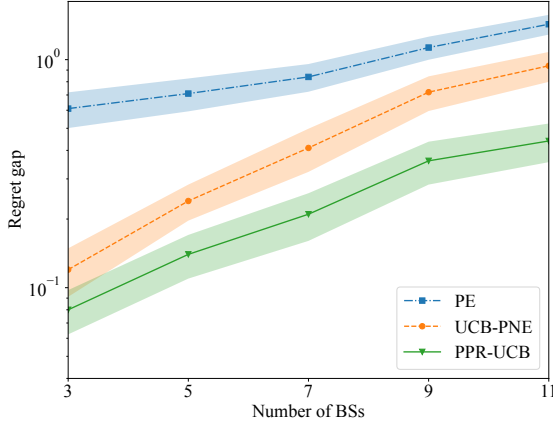


Fig. 4. Regret gap against the number of BSs N for PE (blue dash-dotted line), UCB-PNE (orange dashed line), and PPR-UCB with parameter $\delta = 0.05$ (green solid line).

and plot the regret gap as a function of the number of optimization iterations T . Confirming the discussions in Fig. 2, the proposed PPR-UCB converges to its best achievable dissatisfaction level ϵ closer to the global optimum ϵ^* than all other benchmarks when the number of iterations $T > 40$. These results demonstrate that the provident confidence sets evaluation approach adopted in PPR-UCB accurately captures the residual uncertainty of the utilities and regret for each BS, thus significantly improves the stability of the downlink transmission power allocation process.

Finally, we study the impact of the number of BSs N on the regret gap in Fig. 4. We set the total number of iterations to $T = 200$ for all schemes. The regret gap of PPR-UCB is continuously better than other benchmarks on the increasing size of the cellular network, showing that the proposed PPR-UCB is scalable to strategic games with high dimensional action profiles. One way to further improve the performance of PPR-UCB on higher dimensional action spaces is to increase the size D of the RFFs vector in (14), as this metric adjusts the accuracy of the kernel approximation in (13).

V. CONCLUSION

In this paper, we introduced a centralized BO framework for identifying approximate PNE solutions in a non-cooperative downlink power control game with costly-to-evaluate utility functions. By leveraging martingale techniques to construct confidence sets for the black-box utilities at each BS, the proposed PPR-UCB efficiently converges toward network configurations that approximate PNE solutions. Future work may address theoretical performance guarantees in the forms of game-theoretic regret bounds. Furthermore, it would be interesting to investigate the applications of BO to beam scheduling games [20] or multi-fidelity optimizations in game settings [21].

REFERENCES

- [1] Y. Chen, B. Ai, Y. Niu, K. Guan, and Z. Han, "Resource allocation for device-to-device communications underlying heterogeneous cellular networks using coalitional games," *IEEE Trans. Wireless Commun.*, vol. 17, no. 6, pp. 4163–4176, 2018.
- [2] A. M. Salama, M. Li, L. Lazos, Y. Xiao, and M. Krunz, "Privacy-utility tradeoff in dynamic spectrum sharing with non-cooperative incumbent users," in *Proc. IEEE Int. Conf. Commun. (ICC)*, pp. 1–7, online, 2020.
- [3] X. Zhang, S. Sarkar, A. Bhuyan, S. K. Kasera, and M. Ji, "A non-cooperative game-based distributed beam scheduling framework for 5G millimeter-wave cellular networks," *IEEE Trans. Wireless Commun.*, vol. 21, no. 1, pp. 489–504, 2021.
- [4] Y. Bai, C. Jin, and T. Yu, "Near-optimal reinforcement learning with self-play," in *Proc. Adv. Neural Inf. Process. Syst.*, vol. 33, pp. 2159–2170, online, 2020.
- [5] Z. Li and Y. Luo, "Deep reinforcement learning for Nash equilibrium of differential games," *IEEE Trans. Neural Netw. Learn. Syst.*, vol. 36, no. 2, pp. 2747–2761, 2025.
- [6] D. Shi, L. Li, T. Ohtsuki, M. Pan, Z. Han, and H. V. Poor, "Make smart decisions faster: Deciding D2D resource allocation via Stackelberg game guided multi-agent deep reinforcement learning," *IEEE Trans. Mobile Comput.*, vol. 21, no. 12, pp. 4426–4438, 2021.
- [7] A. M. Nagib, H. Abou-Zeid, and H. S. Hassanein, "Safe and accelerated deep reinforcement learning-based O-RAN slicing: A hybrid transfer learning approach," *IEEE J. Sel. Areas Commun.*, vol. 42, no. 2, pp. 310–325, 2023.
- [8] O. Naparstek and K. Cohen, "Deep multi-user reinforcement learning for distributed dynamic spectrum access," *IEEE Trans. Wireless Commun.*, vol. 18, no. 1, pp. 310–323, 2018.
- [9] P. I. Frazier, "A tutorial on Bayesian optimization," *arXiv preprint arXiv:1807.02811*, 2018.
- [10] Y. Zhang, O. Simeone, S. T. Jose, L. Maggi, and A. Valcarce, "Bayesian and multi-armed contextual meta-optimization for efficient wireless radio resource management," *IEEE Trans. Cogn. Commun. Netw.*, vol. 9, no. 5, pp. 1282–1295, 2023.
- [11] L. Maggi, A. Valcarce, and J. Hoydis, "Bayesian optimization for radio resource management: Open loop power control," *IEEE J. Sel. Areas Commun.*, vol. 39, no. 7, pp. 1858–1871, 2021.
- [12] V. Picheny, M. Binois, and A. Habbal, "A Bayesian optimization approach to find Nash equilibria," *J. Glob. Optim.*, vol. 73, pp. 171–192, 2019.
- [13] S. S. Tay, Q. P. Nguyen, C. S. Foo, and B. K. H. Low, "No-regret sample-efficient Bayesian optimization for finding Nash equilibria with unknown utilities," in *Proc. Int. Conf. Artif. Intell. Stat.*, pp. 3591–3619, Valencia, Spain, 2023.
- [14] 3GPP, "Study on channel model for frequencies from 0.5 to 100 GHz," Tech. Rep. (TR) 38.901, 3rd Generation Partnership Project (3GPP), 2024. Version 17.1.0.
- [15] Z. Dai, B. K. H. Low, and P. Jaillet, "Federated Bayesian optimization via Thompson sampling," in *Proc. Adv. Neural Inf. Process. Syst.*, vol. 33, pp. 9687–9699, Online, 2020.
- [16] J. Ville, *Etude critique de la notion de collectif*. Gauthier-Villars Paris, 1939.
- [17] N. Srinivas, A. Krause, S. M. Kakade, and M. W. Seeger, "Information-theoretic regret bounds for Gaussian process optimization in the bandit setting," *IEEE Trans. Inf. Theory*, vol. 58, no. 5, pp. 3250–3265, 2012.
- [18] S. R. Chowdhury and A. Gopalan, "On kernelized multi-armed bandits," in *Proc. Int. Conf. Mach. Learn.*, pp. 844–853, Sydney, Australia, 2017.
- [19] T. L. Lai and H. Robbins, "Asymptotically efficient adaptive allocation rules," *Adv. Appl. Math.*, vol. 6, no. 1, pp. 4–22, 1985.
- [20] R. Xiong, K. Yin, T. Mi, J. Lu, K. Wan, and R. C. Qiu, "Fair beam allocations through reconfigurable intelligent surfaces," *IEEE J. Sel. Areas Commun.*, vol. 42, no. 11, pp. 3095–3109, 2024.
- [21] Y. Zhang, O. Simeone, and H. V. Poor, "Multi-fidelity Bayesian optimization for Nash equilibria with black-box utilities," *arXiv preprint arXiv:2505.11265*, 2025.